Available online at www.sciencedirect.com
SCIENCE DIRECT®
Cryogenics 44 (2004) 7–14
Cryogenics
www.elsevier.com/locate/cryogenics

Development of vapor-cooled HTS-copper 6-kA current lead incorporating operation in the current-sharing mode

Haigun Lee [a,*], Ho Min Kim [a], Yukikazu Iwasa [a], Keeman Kim [c], Paul Arakawa [b], Greg Laughon [b]

[a] MIT Francis Bitter magnet Laboratory (FBML), Cambridge, MA 02139, USA
[b] American Magnetics, Inc. (AMI), Oak Ridge, TN 37831, USA
[c] Nuclear Fusion R&D Center, Korea Basic Science Institute (KBSI), South Korea

Received 15 May 2003; received in revised form 11 July 2003; accepted 15 July 2003

Abstract

This paper presents the design and performance results of a pair of 6-kA high-temperature superconducting (HTS)-copper current leads, in which, over a short length at the warm end (e.g., 77 K) of each HTS section, comprised of paralleled Bi-2223/Ag–Au tapes, is operated in the *current-sharing* mode. Because of their reliance on vapor cooling, the leads are applicable only to liquid helium-cooled superconducting magnets such as those used in high-energy physics accelerators and fusion machines. The experimental measurements have demonstrated that key performance data of the new 6-kA HTS-copper leads agree reasonably well with those expected from design.

Keywords: High-temperature superconducting (HTS) current lead; Bi-2223/Ag–Au tapes

1. Introduction

Current leads presently available that incorporate high-temperature superconducting (HTS) sections are, though effective in reducing liquid helium boil off rates, bulky and expensive in comparison with copper-based gas-cooled leads. What is needed is a new HTS section that, while keeping efficient thermal performance, results in a compact and affordable lead. Our recent analysis [1] and design/performance [2] have demonstrated that the new HTS sections are compact and thermally efficient. The new HTS/copper leads are applicable only to liquid helium-cooled superconducting magnets such as those used in large high-energy particle accelerators and magnetically confined fusion devices. The new integrated HTS/copper leads that we believe can be made affordable should significantly improve the cryogenic efficiency of these systems. Compactness of the leads should also facilitate retrofitting existing current leads with these new leads.

This paper describes the design procedure, parameters, and performance results of the new 6-kA HTS-copper leads built by AMI and tested at MIT. The leads were designed by MIT based on a new concept described elsewhere [1,2].

2. Design procedure for the HTS section

2.1. Design procedure—Iteration 1

Given below is a step-by-step procedure for design of the HTS section of a new pair of 6-kA HTS-copper leads. In Iteration 1, a protection requirement is not included.

Step 1: Parameters of Bi-2223/Ag–Au tape. Key parameters of Bi-2223/Ag–Au tape are: (1) overall dimensions: width; thickness; and Bi-2223 filling (volume, in %); (2) critical currents in self field: $i_c(T_l)$ where $i_c(T_l)$ is the critical current at the warm end and I_c(@77.3 K and $B_\perp = 0.2$ T) = 80 A and $I_c(T_0)$, similarly at 4.2 K, both at a normal field, $B_\perp = 0.2$ T corresponding to this pair of 6-kA leads; (3) Ag–Au alloy: Au content; cross-sectional area, a_m; T-averaged thermal conductivity, $\tilde{k}_m$,

* Corresponding author.
E-mail address: hlee@jokaku.mit.edu (H. Lee).

0011-2275/$ - see front matter © 2003 Elsevier Ltd. All rights reserved.
doi:10.1016/S0011-2275(03)00182-6

Table 1
Parameters of AMSC Bi-2223/Ag–Au tape

Parameters	Value
Overall width [mm]	4.2
Overall thickness [mm]	0.228
Bi-2223 filling (volume) [%]	42
Au content [wt%]	5.3
Ag–Au cross-section, a_m [mm^2]	0.555
Tape cross-section, a_{tp} [mm^2]	0.958
$i_c(T_l)$ (@77.3 K @$B_\perp = 0.2$ T) [A]	80[a]
$i_c(T_0)$ (@4.2 K @$B_\perp = 0.2$ T) [A]	450[b]
$\tilde{k}_m$ (4.2–77 K) [W/cm K]	0.327
$\tilde{\rho}_m$ (4.2–77 K) [$\mu\Omega$ cm]	1.0

[a] 1-μV/cm criterion.
[b] Note that at 4.2 K the effect of $B_\perp = 0.2$ T is negligible.

in the range T_0–T_l, and T-averaged electrical resistivity, $\tilde{\rho}_m$. Table 1 presents these parameters.

Step 2: Bi-2223/Ag–Au quantity. The number of HTS tape, N_{tp}, is determined by $I_c(T_l) = N_{tp} i_c(T_l)$. Although values of N_{tp} as small as 38 (50%) may be selected for our HTS section, $N_{tp} = 60$, 80% of that ($N_{tp} = 75$) required for a *Fully-Superconducting* (*FullSuper*) version was selected.

Step 3: Current-sharing temperature. Once $I_c(T_l)$ is selected, the current-sharing temperature of the whole HTS' section, T_{cs}, may be determined. For this, it is assumed that $I_c(T) \equiv N_{tp} i_c(T)$ is a linear function of T, decreasing from $I_c(T_0) = N_{tp} i_c(T_0)$ to $N_{tp-c}(T_l)$. From this linear function, we may determine T_{cs}, such that $I_t = I_c(T_{cs})$, where I_t is the transport current.

Step 4: Design of FullSuper version. First, design a *FullSuper* counterpart for a given combination of heat input Q_{in} and length l. In a *FullSuper* counterpart, the entire HTS section operates in the superconducting state at its rated current. Q_{in} and l are related by [1]:

$$Q_{in} = \frac{\tilde{k}_m A_m h_L}{\widetilde{C}_p l} \ln\left[\frac{\widetilde{C}_p (T_l - T_0)}{h_L} + 1\right] \tag{1}$$

where h_L and $\widetilde{C}_p$ are the helium latent heat of vaporization and the heat capacity of helium, respectively. In Eq. (1), A_m is the total cross-sectional area of the Ag–Au alloy, given by $A_m = N_{tp} a_m$. With $h_L = 20.4$ J/g (liquid helium at 4.2 K); $\widetilde{C}_p = 5.280$ J/g K (helium vapor, 4.2–80 K); $T_0 = 4.2$ K; and $T_l = 77.3$ K, a value of Q_{in} may be computed from Eq. (1) for a given choice of l. For $l = 19.5$ cm, $Q_{in} \geqslant 0.065$ W at 6-kA. Because for standard AMI vapor-cooled copper leads rated at 6-kA, $Q_{in} \approx 7.2$ W/lead, reduction in Q_{in} achievable with HTS-copper leads can exceed a factor of 100.

Step 5: Protection criterion. Before proceeding further, it is appropriate at this point to introduce a protection criterion in the design. Here we review a fault-mode scenario (flow stoppage) for protection of a vapor-cooled current lead.

We may analyze this scenario by assuming the adiabatic condition in which Joule heating is converted to raising the lead temperature [3]:

$$\tilde{\rho}_m(T) J_m^2(t) = C_{tp}(T) \frac{dT(t)}{dt} \tag{2}$$

where $\tilde{\rho}_m(T)$ and $J_m(t)$ are, respectively, the resistivity and current density of the matrix; $C_{tp}(T)$ is the heat capacity of the tape (Bi-2223 and Ag–Au); and $T(t)$ is the matrix temperature. Within an order of magnitude, we may assume *volumetric* heat capacities of Bi-2223 and Ag to be equal. With the 58%/42% = 1.38 to take into account the volumetric ratio of this tape, we may assume $C_{tp}(T) \approx 1.38 C_m(T)$ where $C_m(T)$, is the silver heat capacity and integrate Eq. (2) over time and temperature as given below:

$$\int J_m^2(t)\,dt \cong 1.38 \int_{T_i}^{T_f} \frac{C_m(T)}{\tilde{\rho}_m(T)}\,dT \cong 1.38 \frac{\Delta H_m(T_i, T_f)}{\tilde{\rho}_m} \tag{3}$$

where $\Delta H_m(T_i, T_f)$ is the total change in enthalpy of the matrix between T_i (cold) and T_f (warm). The approximation from the middle expression to the last expression in Eq. (3) is valid for alloys whose resistivity is nearly constant over this temperature span. The left-hand side of Eq. (3) may be divided into two time segments, first between $t = 0$ (start of flow stoppage) and $t = \tau_{del}$ (delay in discharge action), and second between $t = \tau_{del}$ and $t = \tau_{del} + \tau_{dis}$, where τ_{dis} is the exponential discharge time constant. From Eq. (3), we may derive a protection criterion for an HTS section:

$$J_{mo}^2 \tau_{del} + \frac{1}{2} J_{mo}^2 \tau_{dis} \leqslant 1.38 \frac{\Delta H_m(T_i, T_f)}{\tilde{\rho}_m} \tag{4}$$

where $J_{mo} \equiv I_t / A_m$ is the matrix current density at $t = 0$.

We apply Eq. (4) to the *FullSuper* HTS section, which for $A_m = 60 a_m = 0.333$ cm^2 has a value of $J_{mo} = 18.02$ kA/cm^2. Thus, the left-hand side of Eq. (4), for $\tau_{del} = 5$ s and $\tau_{dis} = 25.6$ s, for example, equals 57.8×10^8 A^{2}s/cm^4. The values of 5 and 25.6 s, respectively for τ_{del} and τ_{dis}, corresponds to those specified by FNL for vapor-cooled 6-kA all-copper current leads.

With $T_i = 77$ K, $T_f = 293$ K, and $\tilde{\rho}_m = 1 \times 10^{-6}\ \Omega$ cm, the right-hand side of Eq. (4) equals 3.6×10^8 A^{2}s/cm^4 for the enthalpy and density of silver. Clearly, the protection criterion by Eq. (4) is *not* met even with the *FullSuper* version rated at 6 kA.

2.2. Design procedure—Iteration 2

Step 0: Parameters of Bi-2223/Ag–Au tape. The parameters of Bi-2223/Ag–Au tape are identical to those in the Iteration 1 design given in Table 1.

Step 1: Protection requirement—left-hand side of Eq. (4). Because even the total matrix cross-sectional area of 0.333 cm^2 for the *FullSuper* HTS section is inadequate to

satisfy the condition of Eq. (4) (6-kA), it is necessary to introduce, in each HTS section, an additional normal metal (NM) element, thereby reducing J_{mo}. The total NM cross-section area, A_{nm}, may be determined from Eq. (4). By neglecting A_m, we may express the left-hand side of Eq. (4) thus:

$$\left(\frac{I_t}{A_{nm}}\right)^2 \tau_{del} + \frac{1}{2}\left(\frac{I_t}{A_{nm}}\right)^2 \tau_{dis} = \left(\frac{I_t}{A_{nm}}\right)^2 \left(\tau_{del} + \frac{1}{2}\tau_{dis}\right) \tag{5}$$

Right-hand side of Eq. (3). The normal metal must have the following properties.

1. Low T-averaged electrical resistivity, $\tilde{\rho}_{nm}$. Note that a low value of $\tilde{\rho}_{nm}$ will enhance the right-hand side of Eq. (4).
2. Low T-averaged thermal conductivity, $\tilde{k}_{nm}$. Note that $\tilde{k}_{nm}$ will appear in a new expression for Q_{in} similar to Eq. (1).
3. Common material and readily available in tape form.
4. Easily solderable to Bi-2223/Ag–Au tape.

The normal metal selected is a commercial-grade bronze with the following properties.

1. $\tilde{\rho}_{nm} = 2.84 \times 10^{-6}$ Ω cm in the range 77–293 K; 2.25×10^{-6} Ω cm (4.2–77 K) [4].
2. $\tilde{k}_{nm} = 0.35$ W/K cm in the range 4.2–77 K.

Approximating commercial-grade bronze (Cu–Zn) as copper from the standpoint of enthalpy and density, we obtain for $T_i = 77$ K and $T_f = 293$ K:

$$\left(\frac{I_t}{A_{nm}}\right)^2 \left(\tau_{del} + \frac{1}{2}\tau_{dis}\right) \leqslant 1.14 \times 10^8 \ [\mathrm{A^2 s/cm^4}] \tag{6}$$

With $\tau_{del} = 5$ s and $\tau_{dis} = 25.6$ s, $A_{nm} = 2.37$ cm^2 for the 6-kA lead. This value is applicable to each of the new 6-kA HTS-copper leads built by AMI and tested at MIT.

Step 2: Bi-2223/Ag–Au quantity. The numbers of tapes in a *FullSuper* version and the new 6-kA leads are the same as those of the Iteration 1 design.

Configuration. Because this extra NM element required by protection should also be vapor-cooled and because Bi-2223/Ag–Au is in the form of paralleled tapes, the extra NM element too should be in the form of paralleled tapes, each NM tape soldered preferably to each superconductor (SC) tape to enhance heat exchange performance.

Dimensions of NM tape. A thickness of 0.445 mm and a width of 4.45 mm is chosen for each NM tape.

Step 3: Current-sharing temperature. This step is identical to that in Iteration 1. For the 6-kA HTS-copper leads, T_{cs} is 72.1 K. For *FullSuper* versions, T_{cs} is always at 77.3 K, because, by definition, no current-sharing regions exist in the *FullSuper* versions.

Step 4: FullSuper version. With this normal metal included, Eq. (1) is modified to:

$$Q_{in} = \frac{\left(\tilde{k}_m A_m + \tilde{k}_{nm} A_{nm}\right) h_L}{\widetilde{C}_p l} \ln\left[\frac{\widetilde{C}_p (T_l - T_0)}{h_L} + 1\right] \tag{7}$$

Eq. (7) gives: $Q_{in} = 0.56$ W for 6-kA, nearly 10 times greater than that computed in the Iteration 1 design. The new values of Q_{in} are still less than 1/10 those of corresponding AMI standard 6-kA vapor-cooled copper leads.

Step 5: Current-sharing regime. The current-sharing regime spans from $z = l_{cs}$ to $z = l$ (T_0 is at $z = 0$ and T_l at $z = l$). Normalized to l, z becomes ξ, l, to 1, and l_{cs} to ξ_{cs}. ξ_{cs} may be determined by satisfying the following equation, in which the only unknown is ξ_{cs} for a given set of α_{cs} and β_{cs} defined below [1]:

$$\exp\left[\frac{\alpha_{cs}}{2\xi_{cs}}\right] \sin\left[\frac{\beta_{cs}(1-\xi_{cs})}{\xi_{cs}}\right] = \frac{\beta_{cs}(\exp[\alpha_{cs}] - 1)(T_l - T_{cs})}{\alpha_{cs} \exp\left[\frac{\alpha_{cs}}{2}\right](T_{cs} - T_0)} \tag{8}$$

where

$$\alpha_{cs} \equiv \frac{\dot{m}_{he} \widetilde{C}_p l_{cs}}{(\tilde{k}_m A_m + \tilde{k}_{nm} A_{nm})} = \ln\left[\frac{\widetilde{C}_p (T_{cs} - T_0)}{h_L} + 1\right] \tag{9}$$

where $\dot{m}_{he}$ is the helium mass flow rate. Because of the presence of the normal metal element, β_{cs} is modified [1]:

$$\beta_{cs} = \sqrt{\frac{\tilde{\rho}_m \tilde{\rho}_{nm} I_t (I_t - I_{cl})}{(\tilde{k}_m A_m + \tilde{k}_{nm} A_{nm})(\tilde{\rho}_m A_{nm} + \tilde{\rho}_{nm} A_m)(T_l - T_{cs})} - \frac{1}{4}\left(\frac{\dot{m}_{he} \widetilde{C}_p}{\tilde{k}_m A_m + \tilde{k}_{nm} A_{nm}}\right)^2} \tag{10}$$

Step 6: HTS section length. The total HTS section length, l, may be obviously given by $l = l_{cs}/\xi_{cs}$, where ξ_{cs} is determined from Eq. (8) and l_{cs} is determined from Eq. (9) for a given value of $\dot{m}_{he}$, which is equal to Q_{in}/h_L.

Step 7: Heat exchange requirements. Stable operation of a vapor-cooled lead, HTS section or copper section, is possible only when the total required cooling power is properly heat-exchanged with the active element of the lead. A parameter that can gauge heat exchange performance is an effective cooling flux, q_{ef}, in the lead. q_{ef} may be given by the total cooling power divided by the total surface area of the element exposed to cooling. Based on performance of standard AMI vapor-cooled copper leads, q_{ef} value 100 mW/cm^2 or less are considered adequate.

For each HTS section, q_{ef} may be given by:

$$q_{ef} = \frac{\dot{m}_{he} \widetilde{C}_p (T_l - T_0)}{N_{tp} l w_{nm}} \tag{11}$$

where w_{nm} is the NM tape width. In Eq. (11), it is assumed, to enhance heat exchange (or to reduce q_{ef}), that each SC (superconductor) tape is soldered to an NM tape; each NM tape may thus be regarded as a fin to the SC tape. Note that in Eq. (11), to be conservative, $N_{tp} l w_{nm}$, which represents one *half* of the total surface of

NM tapes theoretically exposed to the cooling vapor, is used to compute q_{ef}. The values of q_{ef} computed, 20.2 mW/cm^2, are well below ~100 mW/cm^2. If q_{ef} values turn out to be greater than ~100 mW/cm^2 then it may require another iteration process.

3. Parameters of 6-kA HTS/copper leads

Table 2 presents key parameters of 6-kA HTS sections based on the Iteration 2 design: *FullSuper* in column 2 and the new HTS section in column 3. The table shows that the amount of HTS tape required by the new lead, for the same Q_{in} as that of the *FullSuper* versions, is 80% of that required by the *FullSuper* version related at the same current.

As inferred from the table, tape length becomes shorter as N_{tp} is reduced—more saving of SC is possible. Because q_{ef} is essentially determined by A_{nm}, which in turn is dictated by protection requirements, it is possible to reduce N_{tp} even further than 50% without violating either protection or heat-exchange requirements. There have been other attempts to save the amount of SC in HTS current leads [5].

Table 2
6-kA HTS sections—Iteration 2

Parameter	*FullSuper*	New HTS
# Tapes, SC and NM (N_{tp})	75	60
$I_c(T_l)$ (@77.3 K) [kA]	6	4.8
Ag–Au area, A_m [cm^2]	0.417	0.333
Q_{in} [W]	0.56	
NM tape area, A_{nm} [cm^2]	2.37	
T_{cs} [K]	77.3	72.1
L [cm]	19.5	19.5
l–l_{cs} [mm]	0	4.6
$\tilde{\rho}_m$; $\tilde{\rho}_{nm}$ [μΩ cm]	1.0; 2.25	
$\tilde{k}_m$; $\tilde{k}_{nm}$ [W/K cm]	0.327; 0.35	
NM tape width[a] [mm]	4.45	4.45
Cooling flux [mW/cm]	20.2	20.2
Required HTS tape amount[b]	1	0.80

[a] For tape thickness of 0.445 mm.
[b] Normalized to *FullSuper*.

Table 3
6-kA copper section

Parameters	Value
Operating range [K]	77–293
Active area, A_{cu} [cm^2]	1.19
Active length, l_c [cm]	38
Cooling area [cm^2]	12,650
Cooling mass flow rate	
LN_2, $\dot{m}_{fl}$ [g/s]	0.96
$\dot{m}_{fl}\tilde{C}_{fl}\theta_l$ [W]	216
Effective heat flux	
q_{ef} [mW/cm^2]	17

Table 3 presents key parameters of the copper section of the new 6-kA HTS-copper lead. Note that this lead has $Q_{in} \approx 7.2$ W at the 77-K cold end, which, when divided by $h_L = 20.4$ J/g (latent heat of vaporization of helium), gives $\dot{m}_{he} = 0.353$ g/s. Since LN_2's latent heat of vaporization is 199.3 J/g, its contribution is included in the cooling power and we have: $\dot{m}_{fl} \approx 0.96$ g/s.

4. Experimental setup & procedure

4.1. Cryogenics

Fig. 1 shows a schematic diagram for both He and N_2 flow lines in the experimental setup. For the sake of clarity, only the flow lines for one lead are shown.

Helium. At the start of the experiment, with the test cryostat's outer LN_2 reservoir filled, LHe was transferred into the cryostat. The LHe was filled up to a level just below the HTS/bus–bar junction. Because of a relatively large diameter of the LHe section of the cryostat, 1 cm of LHe level corresponds to ~0.8 l of liquid. It was possible to remove the transfer line from the cryostat after filling was completed.

As shown in Fig. 1, effluent helium vapor from the bath was forced through the paralleled HTS sections, leaving from the top ends of the HTS sections at ~77 K. The 77-K vapor expelling from each HTS section was guided through a stainless pipe, remaining relatively cold from the top end of the cryostat. The cold vapor was heat-exchanged with the ambient and the two separate flows from each HTS sections joined before introduced to a vapor volume flow meter to then exhaust from the system.

The total boil-off rate of LHe for computation of heat input to the LHe bath was measured from change in fluid level, indicated by an AMI level sensor installed in the system. The vapor volume flow meter reading, because of its strong dependence on vapor temperature, is not suitable for accurate determination of heat input.

Nitrogen. LN_2 was introduced at the bottom end of each copper section. The exhaust vapor from the top end of each section was heat-exchanged with the ambient before it was passed through a flow rate meter. The rate of LN_2 flow in each copper section was adjusted to make a vapor flow rate to be near 100 ft^3/h, which corresponds to a designed LN_2 flow rate of 4.3 l/h.

4.2. Electrical

Fig. 1 also shows a schematic diagram for the system's electrical requirements for one lead (+). As indicated in the figure, two current ranges were used for measurement: (1) 0–1000 A and (2) 0–6000 A.

The lead current was measured through the output voltage of either one of the power supplies. Voltages

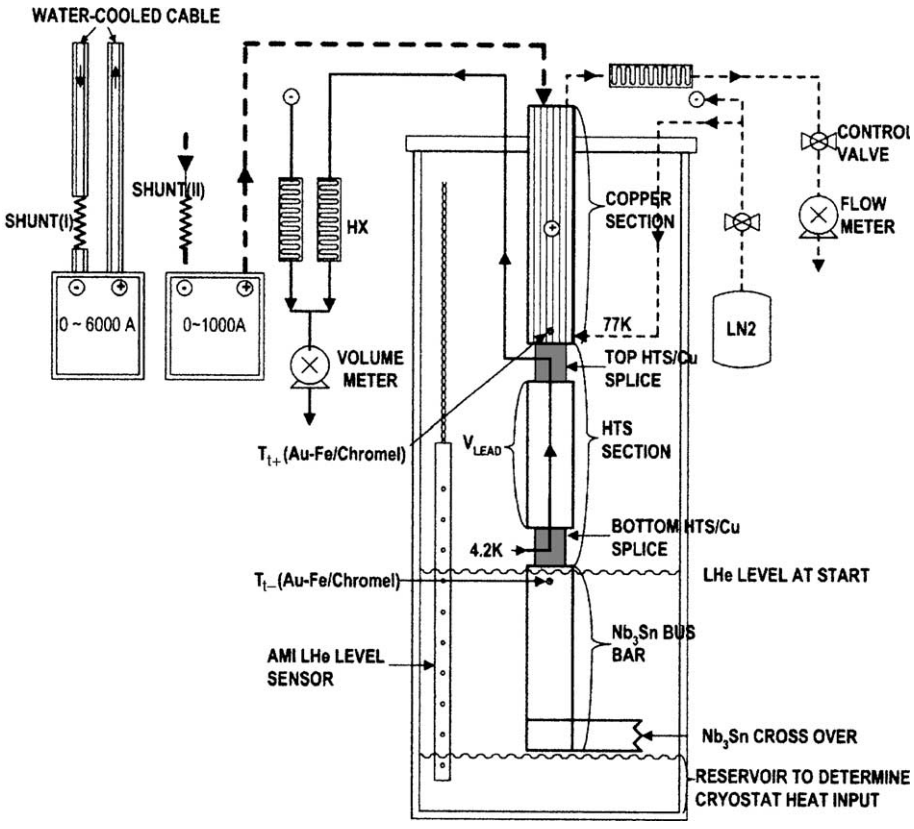

Fig. 1. Schematic diagram for both He and N_2 flow lines in the experimental setup and the system's electrical requirements for one lead (+). As indicated in the figure, two current ranges were used for measurement: (1) 0–1000 A and (2) 0–6000 A. For the sake of clarity, only the flow lines for one lead are shown.

measured for each HTS section include: (1) $V_{\text{lead}}(I)$; (2) thermocouple (Au–Fe/chromel) outputs near the top and bottom HTS/Cu splices; and (3) output voltage from the AMI level sensor.

4.3. New 6-kA HTS-copper leads

Fig. 2 shows a photograph of a pair of 6-kA HTS-copper leads, each comprised of: (1) copper lead (77 K-RT); (2) HTS section (4.2–77 K); (3) Cu/Nb_3Sn composite bus bar (~4.2 K); (4) coolant (liquid N_2) inlet pipes; and (5) He-vapor exhaust pipes. Note that the helium and nitrogen are not mixed. Each HTS section was extended at its cold end with a 30.6-cm long Nb_3Sn/copper composite bus bar. The bus bar, immersed in liquid helium over most of its length during operation, was shunted at the other end with Nb_3Sn tape to its companion bus bar.

5. Results and discussion

5.1. Experimental determination of $Q_{in}(I)$

The total heat input to the LHe in the test cryostat, $Q_{\text{tt}}(I)$, comprise two components: (1) $2Q_{\text{in}}(I)$, the total heat due to the two 6-kA leads (a factor of 2 for the two HTS sections); and (2) extraneous sources of heat, expressed as Q_{ex}, which unlike $Q_{\text{in}}(I)$, is assumed to be independent of I. In the experiment, $\dot{m}_{\text{he}}(t)$ was determined from the time rate of change of the liquid helium level, $\mathrm{d}z_{\text{he}}/\mathrm{d}t$, measured with an AMI level sensor. Thus:

$$\dot{m}_{\text{he}}(I) = -A_{\text{lq}}\tilde{\rho}_{\text{lq}}\frac{\mathrm{d}z_{\text{he}}}{\mathrm{d}t} = \frac{Q_{\text{tt}}}{h_{\text{L}}} = \frac{2Q_{\text{in}}(I) + Q_{\text{ex}}}{h_{\text{L}}} \tag{12}$$

The negative sign is required because the $\mathrm{d}z_{\text{he}}/\mathrm{d}t$ is negative. Where A_{lq} and $\tilde{\rho}_{\text{lq}}$ are, respectively, cross-sectional area of the liquid helium in the cryostat and the liquid helium density at 4.2 K. It is quite accurate to assume $A_{\text{lq}} = A_{\text{cy}}$ where A_{cy} is the test cryostat cross-sectional area. Solving Eq. (12) for $Q_{\text{tt}}(I)$, we obtain:

$$Q_{\text{tt}}(I) = -h_{\text{L}}A_{\text{lq}}\tilde{\rho}_{\text{lq}}\frac{\mathrm{d}z_{\text{he}}}{\mathrm{d}t} \tag{13}$$

5.2. Boil-off and other dissipation data

Fig. 3 shows raw data obtained with the new 6-kA HTS-copper leads tested up to a transport current of 6000 A. Each set of data is discussed briefly.

Closed circles. The closed circles correspond to Q_{tt}, which comprises $2Q_{\text{in}}(I)$ and Q_{ex}.

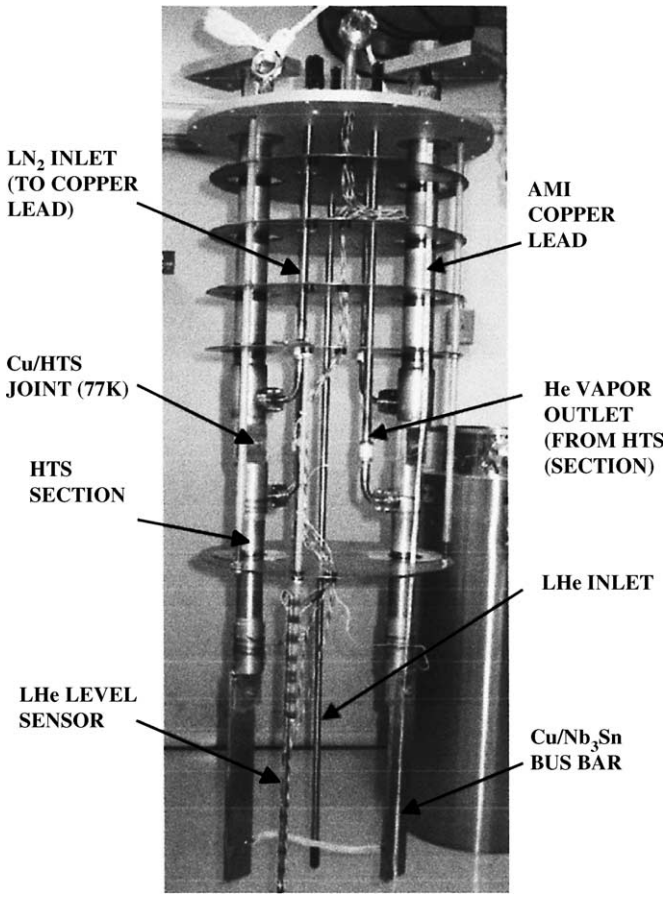

Fig. 2. Photograph of a pair of 6-kA HTS-copper leads, each comprised of: (1) copper lead (77 K-RT); (2) HTS section (4.2–77 K); (3) Cu/Nb_3Sn composite bus bar (~4.2 K); (4) coolant (liquid N_2) inlet pipes; and (5) He-vapor exhaust pipes.

Shadow zone. The shadow zone represents Q_{ex} of the test cryostat. This was determined with $I = 0$ and *after* the LHe level in the test cryostat had dropped below the Nb_3Sn shunt at the bottom of the HTS extension. With no part of the 6-kA HTS-copper leads below the LHe level, Q_{ex} clearly does not contain conductive heat contribution of the leads.

V_{lead} vs. I *curves*. Each of the two VI curves, LEAD(+) and LEAD(−), represents dissipation at the HTS/copper splices, one—at the top and an other—at the bottom end of each HTS section. Note that even the bottom splices were always above the LHe during measurement. At 6000 A, the two splices of each HTS section generates ≈2.75 W or a total of 5.5 W. Because the *measured* Q_{tt} at 6000 A was 2.9 W, clearly most of 5.5 W did not enter into the LHe bath. However, since each bottom end splice is thermally well connected to its respective cold-end extension, a fraction of ~1.4 W (≈2.75/2 W) might have easily entered into the bath. We believe this is responsible for a slight departure of the measured Q_{tt} from 2.5 W for $I > 2000$ A.

Fig. 4 shows $V(I)$ plot over the range 0–1000 A across one HTS section that includes both the top and bottom HTS/copper splices. Because over this current range the HTS is superconducting, a combined total resistance, 60 nΩ, for this HTS section, may be considered due almost entirely to the two splices.

Fig. 5 shows $V(I)$ plots in the range 0–6000 A for the two HTS sections. For each curve the dashed line corresponds to V due to the two HTS/copper splices. The departure from this dashed line demonstrates appearance of the current-sharing region in the HTS section. Although each of 60 AMSC Bi-2223/Ag–Au tapes has an I_c specification of 100 A (77 K; *self field*), a combination of variation in I_c received from AMSC and degradation in I_c incurred during the brass strip soldering process resulted in a large variation in I_c (77 K; *self field*), as low as 60 A and some as high as 120 A. I_c is further depressed by another 20% when the effect of $B_\perp = 0.2$ T is included. Therefore, it is not surprising to observe the current-sharing region occurring at a total current of ~2200 A for the "+" section and ~2500 A for the "−" section.

5.3. Temperature data

The measured temperatures of both the bottom and top end of each HTS section, within an experimental

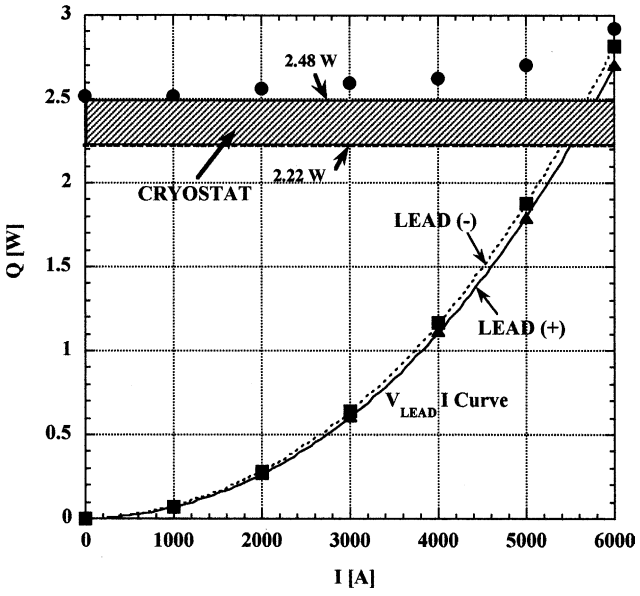

Fig. 3. Raw data. The closed circles correspond to $Q_{tt}(I)$. The shadow zone represents the measured range of Q_{ex}. Each $V_{lead} \times I$ curve represents dissipation due chiefly to the splice resistances at the top and bottom HTS/copper couplings in each HTS section.

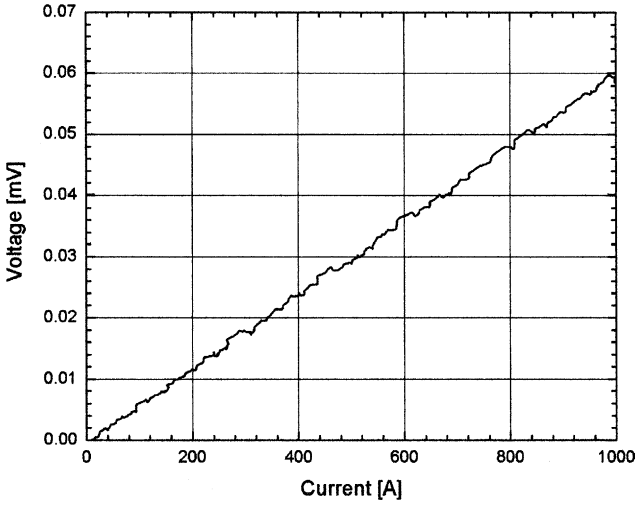

Fig. 4. $V(I)$ plot in the 0–1000 A range across one HTS section containing both top and bottom HTS/copper splices, within this range, HTS section is superconducting and the voltage is due almost entirely to the two splices, which has a combined effective resistance of 60 nΩ.

uncertainly of ~0.5 K, were independent of current and remained, respectively, at 4.2 and 77 K.

5.4. LN_2 supply rate

Each copper section was supplied with LN_2 at a flow rate roughly equal to 0.96 g/s (4.3 liquid l/h), which is equivalent to a room-temperature vapor flow rate of ~100 ft^3/h. Indeed, the LN_2 supply rate was set to make

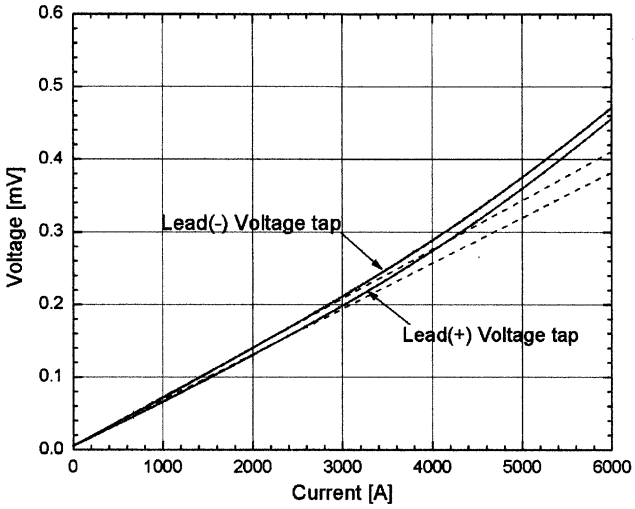

Fig. 5. $V(I)$ plots in the 0–6000 A range across both HTS sections, each containing both top and bottom HTS/copper splices. The dashed line for each plot corresponds to purely resistive contribution from the splices. The departure from each dashed line just indicates the current-sharing region in each HTS section.

the outlet vapor flow rate to be ~100 ft^3/h during the measurement.

5.5. Discussion of results

We may derive the following results from the data obtained.

- From Fig. 3, we may extract $2Q_{in} \leqslant 0.28$ W given by $Q_{tt}(0) = 2.5$ W subtracted by the minimum extraneous heat input, $Q_{ex} = 2.22$ W or $Q_{in} \leqslant 0.14$ W. Because the design value for $Q_{in} = 0.56$ W, measured Q_{in} is 1/4 of the design value. Two parameters appearing in Eq. (5) that were not measured or known accurately are $\tilde{k}_m$ and $\tilde{k}_{nm}$ the temperature-averaged thermal conductivities, respectively, of the Ag–Au substrate and brass. We therefore attribute this "pleasant" discrepancy (Q_{in} measured $< Q_{in}$ design) to the uncertainties in the value of both $\tilde{k}_m$ and $\tilde{k}_{nm}$.
- $2Q_{in}(I)$ is nearly independent of I—a slight increase, i.e., 0.4 W $[= 2Q_{in}(6000\text{ A}) - 2Q_{in}(0)]$, observed in the experiment is due chiefly to a fraction of a large dissipation taking place at the bottom HTS/Cu splice in each HTS section. As pointed out above, at 6000 A, the bottom HTS/Cu splice of each section is generating ~1.4 W or a total of ~2.8 W. Because each bottom splice is thermally well connected to its Nb_3Sn bus bar extension, it is reasonable to assume a fraction of it, ~0.2 W/section, enters into the LHe bath, thus making $2Q_{in}$ increase slightly with I.
- The temperatures of both the bottom and top ends of each HTS section are independent of I and remain, respectively, at ~4.2 K and ~77 K.

- As designed, unlike a *FullSuper* counterpart in which the HTS tapes operate in the fully superconducting state, $V(I)$ plots shown in Fig. 5 clearly show that the HTS tapes in each HTS section of this new pair of leads operate partially in the current-sharing mode. Because in an inevitable variation in $I_c(T_l)$ among 60 individual tape, each soldered with a brass strip, transition to the current-sharing region is not as defined as it would be if the values of $I_c(T_l)$ of 60 tapes were identical.

As may be inferred from Fig. 5, at 6000 A, resistive voltages due to the HTS tapes are 70 μV for the "+" section and 50 μV for the "−" section. In total these voltages generate 0.72 W. Since $2Q_{in}(6000\ \mathrm{A}) - 2Q_{in}(0)$ is only 0.4 W even after attributing this to the generation at the two bottom HTS/Cu splices, we can confidently conclude that each HTS section successfully removes this "genuine" dissipation in the current-sharing region without increasing the heat input to the LHe as does the design call for.

- LN_2 flow rate required for operation agreed with that given by the design.

6. Conclusions

The experimental measurements have demonstrated that key performance data of the new 6-kA HTS-copper leads agree reasonably well with those expected from design. We conclude that this new pair of 6-kA HTS-copper leads can be a highly promising alternative for high-current leads that incorporate HTS.

Acknowledgement

One of the authors (H.M. Kim) would like to thank Korea Science & Eng. Foundation (KOSEF) for its financial support during his stay as a postdoc fellow at MIT, USA.

References

[1] Iwasa Y, Lee H. High-temperature superconducting current lead incorporating operation in the current-sharing mode. Cryogenics 2000;40:209.
[2] Lee H, Arakawa P, Ef ferson KR, Fielden R, Iwasa Y. AMI-MIT 1-KA leads with high-temperature superconducting section—design concept and key parameters. IEEE Trans Appl Supercond 2001;11(1):2539.
[3] Iwasa Y. Case studies in superconducting magnets. New York: Plenum Press; 1994.
[4] Clark AF, Childs GE, Wallace GH. Electrical resistivity of some engineering alloys at low temperatures. Cryogenics 1970; 10:295.
[5] Gavrilin AV, Keilin VE, Kovalev LA, Kruglov SL, Shcherbakov VI, Akimov II, et al. Optimized HTS current leads. IEEE Trans Appl Supercond 1999;9(2):531.